

Article

# Effects of Deformation Conditions on the Rolling Force during Variable Gauge Rolling

Ehsan Shafiei <sup>1,2,\*</sup>  and Kamran Dehghani <sup>1</sup>

<sup>1</sup> Department of Mining and Metallurgical Engineering, Amirkabir University of Technology, Tehran 158754413, Iran; Dehghani@aut.ac.ir

<sup>2</sup> Department of Materials Engineering, Islamic Azad University, Bandar Abbas Branch, Bandar Abbas, Hormozgan 7915893144, Iran

\* Correspondence: shafiei.ehsan.mse@gmail.com; Tel.: +98-93-7076-2834

Received: 8 June 2018; Accepted: 17 July 2018; Published: 19 July 2018



**Abstract:** In this study, effects of different deformation conditions on the rolling force were studied during variable gauge rolling processes. To this end, variations of rolling forces with rolling times were analyzed at different roll diameters, absolute thickness reductions and friction coefficients. Considering the rolling force variations, an abrupt change in the outlet section of downward and outward rolling was observed at all deformation conditions. The experimental data, along with the results obtained from finite element method (FEM) simulations, revealed that this drop in the rolling force (DRF) is strongly dependent on the deformation conditions. It was found that the DRF value increases with increasing absolute thickness reduction, roll diameter and friction coefficient. Furthermore, dependency of contact length on the roll radius and wedge angle (slope of the thickness transition zone) was investigated. Accordingly, it was concluded that the variations of the DRF value can be mainly attributed to the changes in the contact length during variable gauge rolling. Moreover, slab method analysis was used to model the effects of deformation conditions on DRF.

**Keywords:** variable gauge rolling; flexible rolling; tailor rolled blanks; rolling force

## 1. Introduction

Environmental concerns, safety regulations, and consumer demands are driving the need for a lighter vehicle that is more fuel-efficient, produces lower emissions, and provides improved crash-worthiness and performance reliability [1]. Accordingly, it has become a big challenge for product development teams to create a design that satisfies all the aforementioned expectations. As a result, great attention has been paid to tailor rolled blanks (TRB) with variable thicknesses to produce light weight components in the automotive industry, with popular applications including side frames, doors and pillars [2].

In variable gauge rolling (VGR), new products with variable thicknesses are produced by adjusting the roll gap during the rolling process. Compared to conventional rolling, variable gauge rolling can be divided into three stages: downward rolling, flat rolling and upward rolling. In VGR, the flat regions with a constant thickness are rolled by flat rolling, whereas thickness transition regions with a variable thickness are formed by downward and upward rolling.

Kopp et al. [3] studied the forming behavior of TRBs made from DC04 steel utilizing deep drawing tests. They found out that longer thickness transition zones (TTZs) result in less wrinkling. In addition, Meyer et al. [4] investigated the increase in drawing depth due to the weakening of certain areas using TRBs. They concluded that the TTZ geometry should be determined considering the subsequent forming processes. Hirt et al. [5] studied the spring back behavior of the thick and

thin sides of TRBs by locally moving the die segment towards the punch. Zhang et al. [6] utilized linear Lagrangian interpolation method to estimate the mechanical properties of TTZ at each point. Shafiei and Dehghani [7] studied the effects of thickness ratio and length of TTZ on the tensile behavior of TRBs. They concluded that total elongation of TRBs decreases with decreasing thickness ratio. Furthermore, they found out that increasing length of TTZ has a detrimental effect on the total elongation of TRBs. In a different study, they examined the effects of strength gradient and geometrical inhomogeneity on the total elongation of TRBs. It was concluded that these factors can restrict total elongation of TRBs during uniaxial tension [8].

Despite the attempts for analyzing formability and performance of TRBs [9–13], there are less researches which have been focused on the evaluation of deformation conditions and their effects on rolling force. Zhang et al. [14] presented a solution for the differential equations of force equilibrium for both upward and downward steps of VGR to predict the required rolling force. Liu et al. [15] presented a kinematically admissible velocity field to analyze forward slip during different stages of variable gauge rolling. In both of these studies, the effects of friction coefficient, roll diameter and absolute thickness reduction on variations of rolling force during VGR were not studied. In another study, Yu et al. [16] studied the variations of rolling force during variable gauge rolling by finite elements simulations; however, no experimental data was provided to support the findings. Furthermore, the potential reasons behind these variations during different stages of variable gauge rolling were not discussed.

Since the roll gap is adjusted instantaneously during VGR, it has a great importance to study the variations of rolling force to achieve highest possible dimensions accuracy. Accordingly, the main aim of this investigation is to study the effects of deformation conditions on the variations of rolling force during VGR of DP590. In this regard, the reasons behind the variations of rolling force vs. rolling time during VGR were fully discussed to justify the results for the first time. Furthermore, the existing formulations developed for flat rolling were modified to study rolling force variations during successive stages of VGR.

## 2. Experimental Procedure

In this study, automotive steel DP590 with an initial thickness of 2 mm was used to produce TRBs with variable thicknesses, the chemical composition of which is shown in Table 1. Furthermore, the different mechanical characteristics of DP590 sheets are summarized in Table 2.

**Table 1.** Chemical compositions (Wt %) of DP590.

Elements	C	Si	Mn	Nb	Al	Cr	Fe
Wt %	0.149	0.467	1.513	0.016	0.033	0.23	Bal.

**Table 2.** Mechanical properties of DP590.

	Yield Stress, MPa	Ultimate Tensile Strength, MPa	Young Modulus, GPa	$n$	K, MPa	Total Elongation, %	Uniform Elongation, %
DP590	486 ± 14	731 ± 18	207	0.125 ± 0.02	900 ± 20	27 ± 0.5	19 ± 0.5

TRBs were produced using a four-high mill equipped with VGR technology to adjust the roll gap instantaneously. The roll gap adjustment was carried out using a set of hydraulic cylinders as actuators, a thickness measurement sensor (non-contact measurement using two sensors to sandwich the target) and a tracking device. All processes were controlled by a computer to obtain the target thicknesses with reasonable accuracy. In case of deviation from target values, the hydraulic cylinders were driven to adjust the roll gap. The width of all TRBs and the working roll diameter were 450 mm and 183 mm, respectively.

### 3. Results

Figure 1a,b depicts the variations of the target thickness of TRBs vs. rolling time produced via the VGR process. As shown, two different thickness ratios of 0.89 (1.9 mm  $\leftrightarrow$  1.7 mm) and 0.47 (1.9 mm  $\leftrightarrow$  0.9 mm) were considered to evaluate the effect of thickness reduction on rolling force during the VGR process. Accordingly, to prove the accuracy of the VGR setup, the instantaneous thickness was recorded as shown in Figure 2. Considering the target and real values of thickness, the maximum error associated with thickness changes is about 3.9%, which lies within an acceptable range. In addition, for both cases, the thickness accuracy decreases with increasing reduction after downward rolling due to an increase in rolling force and possible roll deflections.

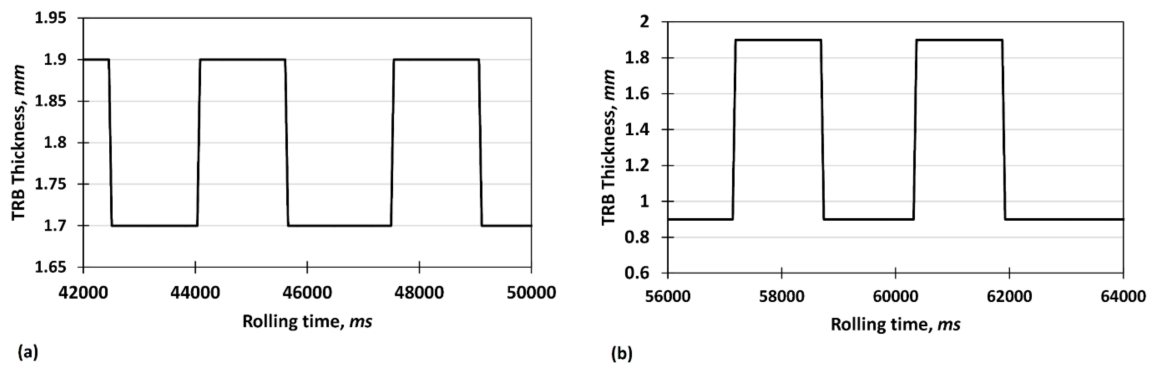


Figure 1. Variations of target thickness with rolling time for (a) absolute thickness reduction of 0.2 mm and (b) absolute thickness reduction of 1 mm.

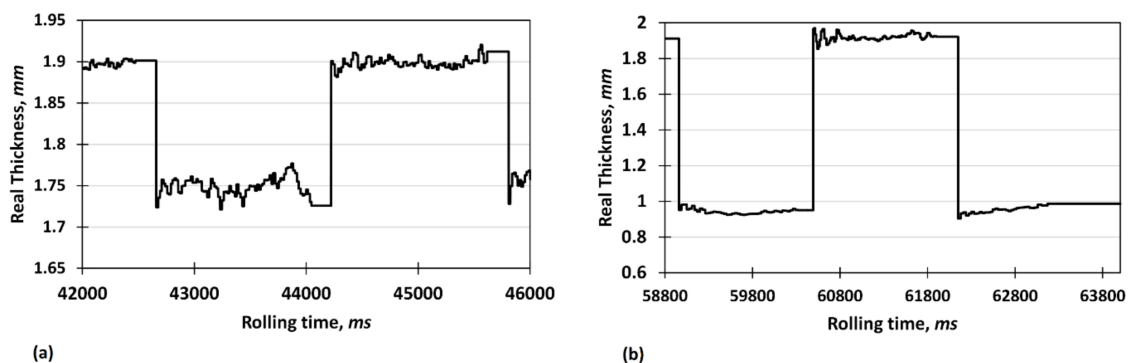
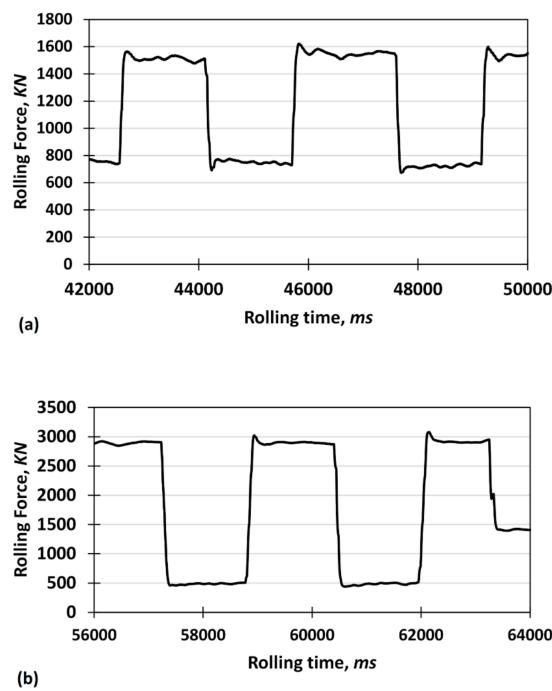


Figure 2. Variations of real thickness with rolling time for (a) absolute thickness reduction of 0.2 mm and (b) absolute thickness reduction of 1 mm.

Figure 3 shows the corresponding rolling force vs. rolling time curves acquired during VGR of TRBs with thickness ratios of 0.89 and 0.47, respectively. It can be seen that the rolling force increases when downward rolling is performed; however, when downward rolling turns to flat rolling, the rolling force experiences a rapid drop. This rapid DRF is also detected when upward rolling turns to flat rolling to produce the thicker side. Furthermore, it is shown that the rolling force changes by a factor of two and six during VGR of the TRBs with thickness ratios of 0.89 and 0.47, respectively. These changes in rolling force can be simply attributed to the amount of thickness reduction and materials plasticity. However, the reason for the abrupt changes in rolling force in the outlet sections of downward and upward rolling is still ambiguous.

In order to evaluate the effects of other important parameters, including roll diameter and friction coefficient on the rolling force during VGR, FEM (finite element method) simulations were carried out. To this end, commercial ABAQUS/Dynamic Explicit software was used to predict the rolling force vs. rolling time curves during VGR at different deformation conditions. In this regard, the Von-Mises yield

surface was applied to model the isotropic metal plasticity. In addition, an eight-node brick element with reduced integration (C3D8R) was used for the blanks, and the rolls were considered as rigid bodies. Furthermore, adaptive re-meshing was performed using the arbitrary Lagrangian-Eulerian (ALE) method to prevent mesh degeneration. The FEM simulations were first applied to estimate the friction coefficient during VGR. Accordingly, the VGR process was simulated with different friction coefficients of 0.14, 0.17 and 0.21 for the condition with a thickness ratio of 0.89. According to the results of simulations shown in Figure 4, the highest degree of accuracy with respect to the experimental data was obtained for the condition with a friction coefficient of 0.17. It is notable to mention that the forward-backward pull tensions were 50 MPa ( $0.1 \times$  yield strength) to prevent sliding between rolls and the workpiece.



**Figure 3.** Rolling force vs. rolling time curves for (a) absolute thickness reduction of 0.2 mm and (b) absolute thickness reduction of 1 mm.

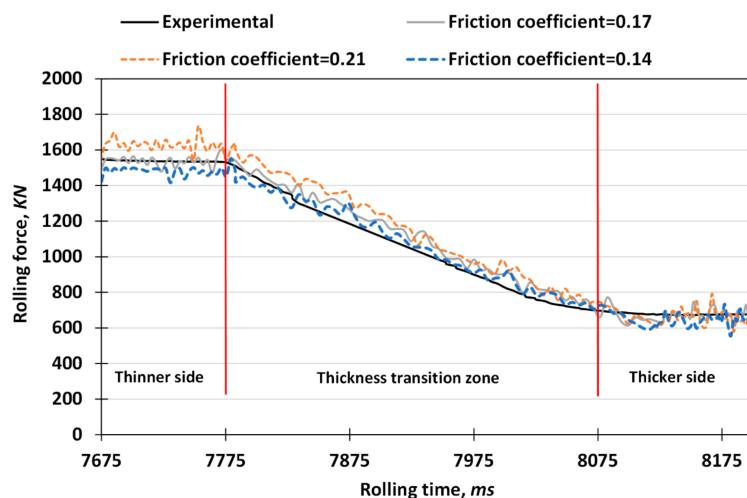


**Figure 4.** Estimation of friction coefficient during VGR.

To study the effects of roll diameter on the rolling force and DRF during VGR, the condition with an absolute thickness reduction of 1 mm and friction coefficient of 0.17 was simulated with three different roll diameters of 130, 183 and 230 mm. Figure 5 depicts the variations of rolling force vs. rolling time during both downward rolling and its subsequent flat rolling with different roll diameters. As shown, the rolling force increases with increasing roll diameters for both rolling stages due to an increase in the contact lengths. Furthermore, Figure 5 also shows that the DRF value increases with increasing roll diameter.

Figure 6 shows the rolling force vs. rolling time curves with different friction coefficients of 0.1, 0.14 and 0.17 and a constant absolute thickness reduction of 1 mm. As expected, the rolling force increases with an increasing friction coefficient. However, this increase becomes more evident in the outlet region of downward rolling due to the fact that the maximum rolling force is obtained in this region.

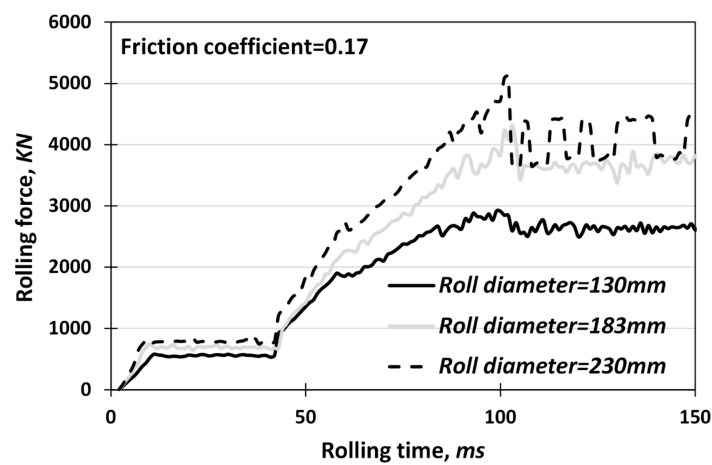


Figure 5. Effect of roll diameter on the rolling force during VGR.

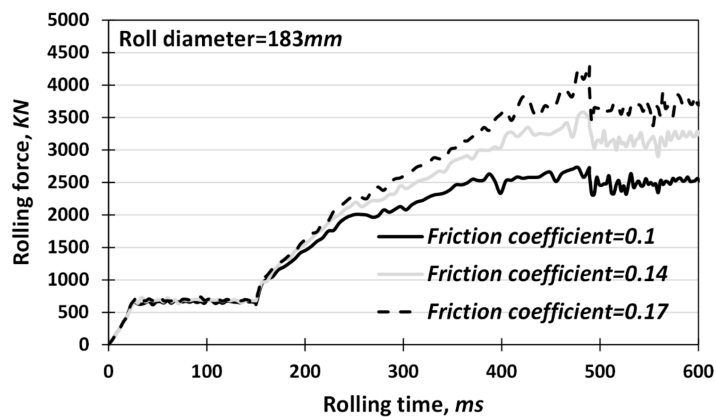


Figure 6. Effect of friction coefficient on the rolling force during VGR.

#### 4. Discussion

Figure 7 shows the variations of rolling force in the outlet section of downward rolling schematically. As shown, due to the occurrence of a DRF, the maximum needed rolling force exceeds the required rolling force needed to obtain the section with maximum absolute thickness reduction (thinner side). Liu et al. [15] reported that this DRF is solely attributed to forward slip.

In order to clarify this issue, the variations of rolling force with time were studied at different reductions in more detail, shown in Figure 8a–d. In downward rolling, the DRF value increases from 63 KN to 164 KN for thickness ratios of 0.89 and 0.47, respectively. Furthermore, in upward rolling,

the DRF values of 77 kN and 48 kN were obtained for the thickness ratios of 0.89 and 0.47, respectively. Accordingly, it can be concluded that in downward rolling, the DRF value increases with increasing thickness reduction and contrarily, in upward rolling, this value decreases with increasing thickness reduction. To justify these results, it is necessary to study the effect of the factors affecting rolling force in three successive sections of the VGR process. Accordingly, the effects of the changes in thickness reduction and roll diameter on the variations of rolling force were taken into account by considering their effects on contact length.

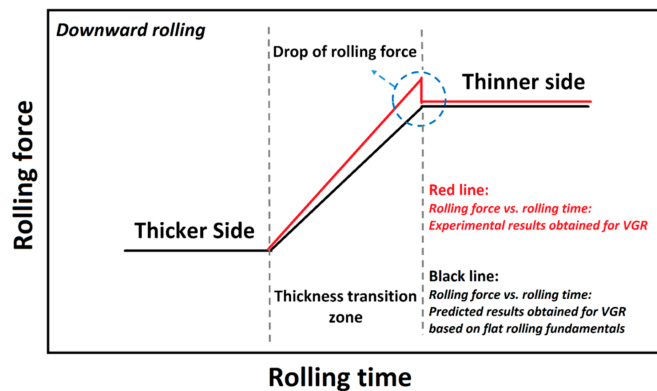


Figure 7. Schematic representation of variations of rolling force vs. rolling time during downward rolling.

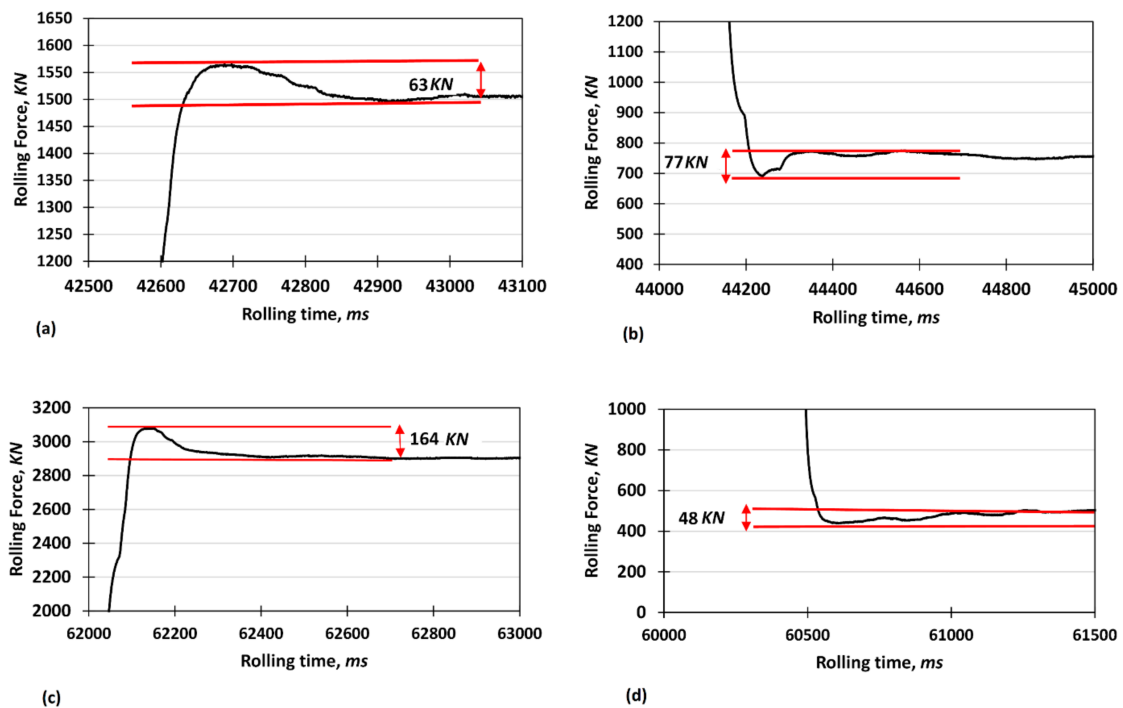


Figure 8. Variations of rolling force with rolling time for (a) downward rolling with absolute thickness reduction of 0.2 mm; (b) upward rolling with absolute thickness reduction of 0.2 mm; (c) downward rolling with absolute thickness reduction of 1 mm; and (d) upward rolling with absolute thickness reduction of 1 mm.

In flat rolling, it is widely accepted that the contact length can be obtained using the following expression [17]:

$$l_d = \sqrt{R\Delta h} \tag{1}$$

where  $R$  and  $\Delta h$  are roll radius and absolute reduction in thickness, respectively. It is notable to mention that the absolute reduction in flat rolling regions was obtained based on the initial thickness of 2 mm.

In contrast to flat rolling, the workpiece is out of touch with the rolls in upward rolling, and consequently the contact angle is smaller than the bite angle of flat rolling. Contrarily, the contact angle increases with increasing wedge angle ( $\varphi$ ) in downward rolling. Accordingly, the contact angle is bigger than the bite angle obtained in the flat rolling of the thicker part. According to the geometry of the deformation zone, the following expression can be used to obtain the contact length during upward and downward rolling:

$$l_{down,up} = \sqrt{(R \sin \varphi)^2 + R \cos \varphi \Delta h - \left(\frac{\Delta h^2}{4}\right)} \pm R \sin \varphi \tag{2}$$

where  $\varphi$  is the wedge angle. It is worth mentioning that the wedge angle is a function of thickness reduction and length of the TTZ. Accordingly, for a constant length of the TTZ, the wedge angle increases with increasing thickness reduction (or decreasing thickness ratio). Figure 9 shows the dependence of contact length during upward and downward rolling for absolute thickness reductions of 0.2 mm and 1 mm, respectively. As shown, the contact length increases sharply with increasing wedge angle during downward rolling. In addition, it is clear that the contact length is more sensitive to the wedge angle for absolute reduction of 0.2 mm as compared to the condition with absolute reduction of 1 mm. Utilizing Equations (1) and (2), the changes in contact length for the studied cases in the outlet sections of the TTZ during downward and upward rolling can be calculated. Accordingly, Figure 10 shows the effect of absolute thickness reduction on the changes of contact length in the outlet section of the TTZ. As depicted, the maximum and minimum values of these changes were obtained for downward and upward rolling with an absolute thickness reduction of 1 mm, respectively.

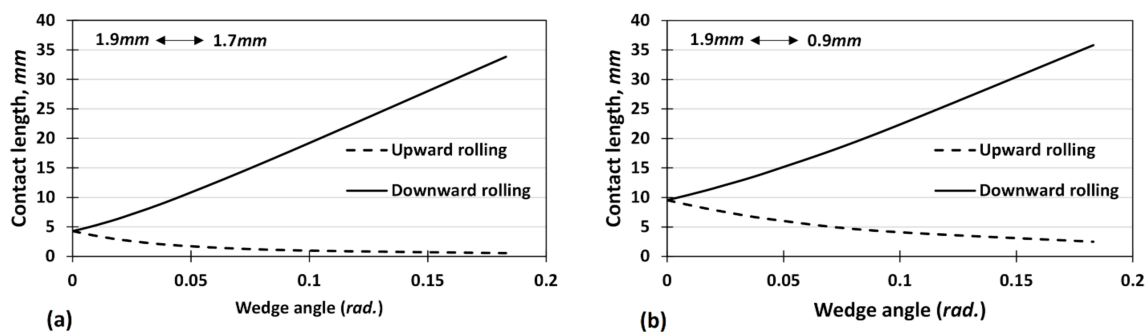


**Figure 9.** Dependency of contact length during upward and downward rolling for (a) absolute thickness reduction of 0.2 mm and (b) absolute thickness reduction of 1 mm.

Since the rolling force is proportional to contact length, it can be concluded that the DRF in the outlet sections can be a function of changes in contact length as well. The variations of DRF in Figure 8a–d prove the aforementioned claim. As expected, the maximum DRF value was obtained for the condition with higher changes in contact length during downward rolling. Similarly, the minimum value of DRF was obtained for the condition with lower changes in contact length during downward rolling. In other words, due to lower values of bite angle for the condition with an absolute thickness reduction of 0.2 mm, the contact length is more sensitive to the wedge angle and decreases more rapidly with an increasing wedge angle. Accordingly, a higher DRF value is obtained for this condition during upward rolling. Consequently, since the rolling force shows an abrupt change to a peak value before turning to flat rolling in downward rolling, it is essential to consider these changes when designing forming tools for VGR to obtain proper thickness accuracy.

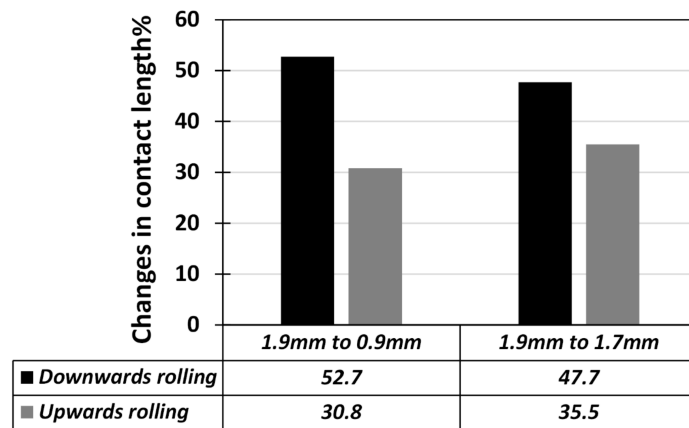


Figure 10. Effect of thickness reduction on the changes in the contact length.

In order to study the reasons behind the dependence of DRF on absolute thickness reduction and contact length in more detail, the slab method was used to model the variations of rolling force in the outlet section of downward rolling. According to the slab method, the rolling pressure required for flat rolling in the plane strain condition can be obtained as follows [17]:

$$P_1 = 1.15\bar{Y} \left( 1 + \frac{\mu_1 l_1}{2h_{avg}} \right) \tag{3}$$

where  $\bar{Y}$ ,  $\mu_1$  and  $l_1$  are average yield stress, friction coefficient and contact length, respectively. The values of  $l_1$  can be obtained using Equation (1). Furthermore,  $h_{avg}$  can be calculated with respect to the thicknesses of the thinner and thicker sides along the longitudinal direction.

Substitution of  $l_1$  with the formulation derived for the VGR process (Equation (2)), Equation (4) can be rewritten to obtain the required rolling pressure during VGR as follows:

$$P_2 = 1.15\bar{Y} \left( 1 + \frac{\mu_2 l_2}{2h_{avg}} \right) \tag{4}$$

Accordingly, the DRF values in the outlet section of downward rolling can be obtained using following expression:

$$DRF = P_2 l_2 w - P_1 l_1 w \tag{5}$$

Substitution of Equations (3) and (4) into Equation (5) leads to the following expression for the DRF:

$$DRF = 1.15\bar{Y} w \left( \Delta l + \frac{1}{2h_{avg}} (\mu_2 l_2^2 - \mu_1 l_1^2) \right) \tag{6}$$

It is widely accepted that the friction coefficient is a reduction-sensitive parameter and may increase with increasing thickness reduction [18]; however, for the sake of simplicity, a constant friction coefficient of 0.17 was applied for different thickness reductions during VGR. Furthermore, as the thickness reduction increases instantaneously along the TTZ, it was impossible to consider the friction coefficient as a reduction-dependent parameter; however, its changes along the rolling direction during VGR can affect the solution accuracy. As shown in Figure 11, the accuracy in the estimation of the rolling force decreases with increasing rolling force (increasing thickness reduction) for both studied friction coefficients of 0.14 and 0.17. This can be mainly attributed to the reduction-dependent characteristic of the friction coefficient. In other words, underestimation of the friction coefficient at higher thickness reductions may result in less accuracy in rolling force estimation by FEM simulations.

Assuming a constant friction coefficient during VGR, the following expression can be obtained for the DRF:

$$DRF = 1.15\bar{Y}w\Delta l \left( 1 + \frac{\mu}{2h_{avg}} (l_1 + l_2) \right) \tag{7}$$

As can be seen from Equation (7), the DRF is directly proportional to the changes in contact length. Accordingly, this can prove the competency of the analyses provided in Figures 9 and 10 regarding effects of thickness reduction on the DRF.

Figure 12 depicts the variations of the DRF as a function of downward rolling contact length ( $l_2$ ) using Equation (7). As shown, a good correlation was obtained between the experimental results and the slab method analysis for an absolute thickness reduction of 1 mm.

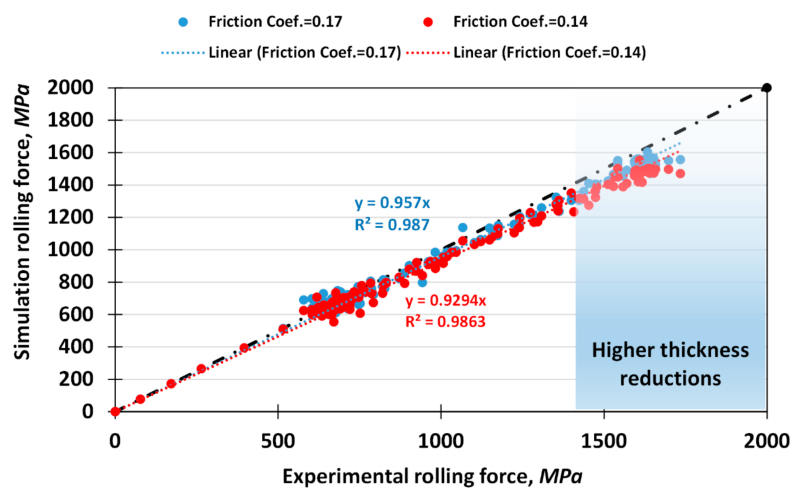


Figure 11. Simulation rolling force vs. experimental rolling force for friction coefficients of 0.14 and 0.17.

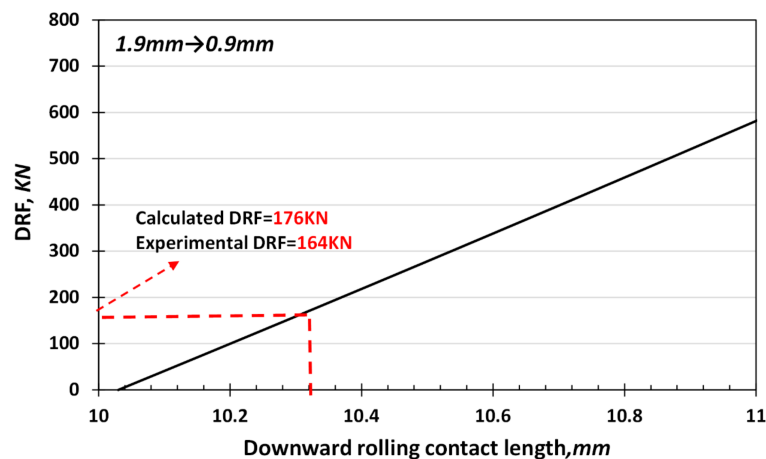


Figure 12. Predicted DRF values using slab method analysis.

Figure 13 shows the variations of contact length as a function of roll radius for the downward and the subsequent flat rolling stages at the aforementioned conditions using Equations (1) and (2). As depicted, the difference between the two contact lengths increases with increasing roll diameters, which leads to higher values of the DRF (See Equation (7)). According to the data provided in Figure 14, and with respect to Equations (1) and (2), it was found that the DRF is a linear function of  $\sqrt{R}$ . The high correlation factor of 0.99 proves the competency of this regression analysis.

In addition, as shown in Figure 15, the rapid changes in the DRF are an exponential function of the friction coefficient. The reason for this phenomenon can be attributed to the changes in the vertical

component of the frictional forces when the downward rolling turns into the subsequent flat rolling. Furthermore, variations of the friction coefficient with thickness reduction may have similar effects on the DRF, as per Equation (7).

In comparison with the results obtained by Yu et al. [16], similar trends were obtained for the variations in the DRF with thickness reduction, roll diameter and friction coefficients. However, the magnitude of these variations are not comparable as their work was not validated with experimental data. Furthermore, they provide no reasons for these variations from a mechanical point of view.

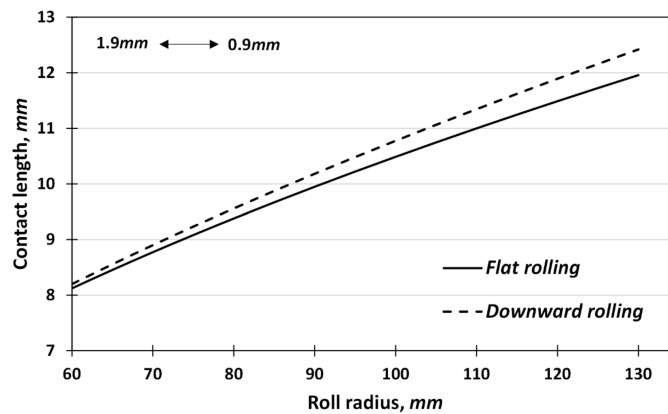


Figure 13. Effect of roll radius on the contact length during VGR.

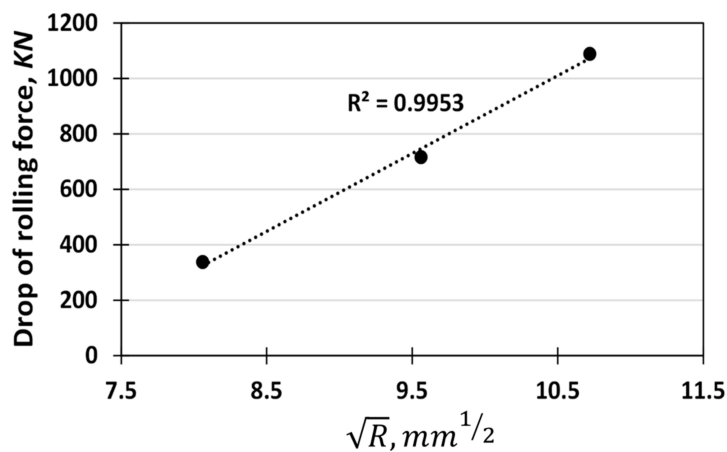


Figure 14. Dependence of DRF on the roll radius during downward rolling.

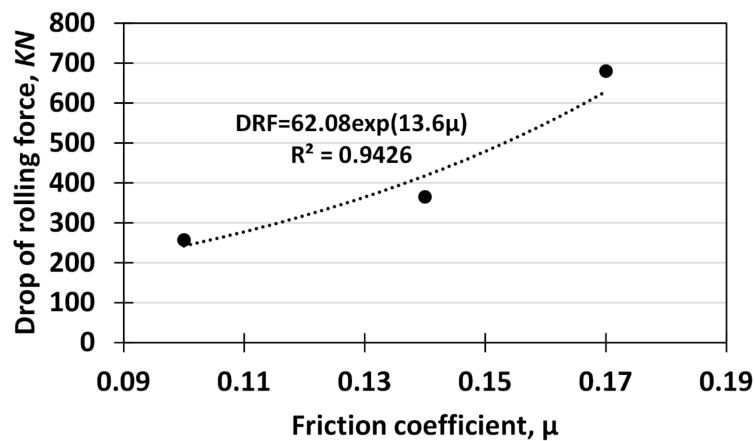


Figure 15. Dependence of DRF on the friction coefficient during downward rolling.

## 5. Conclusions

- The rolling force increases when the downward rolling is performed; however, upward rolling is associated with a continuous reduction in the rolling force.
- An abrupt change in the rolling force in the outlet sections of the downward and upward rolling was observed. It was found that this abrupt change in rolling force is a function of absolute thickness reduction, roll diameter and friction coefficients. This abrupt change in rolling force was called DRF.
- The reasons for these abrupt changes in rolling force were attributed to the changes in contact length and the vertical component of frictional forces.
- The dependence of contact length during downward and upward rolling on the wedge angle and roll diameter of TRBs was studied. It was found that both parameters have a great effect on contact length.
- The experimental data obtained from VGR of DP590 revealed that the abrupt change in the rolling force increases with increasing absolute thickness reduction.
- The data provided using FEM simulations showed that this abrupt change in the rolling force during VGR increases with increasing friction coefficients and roll diameter.

**Author Contributions:** E.S. and K.D. conceived and designed the experiments; E.S. performed the experiments; E.S. analyzed the data; E.S. contributed materials tools; E.S. wrote the paper.

**Funding:** This research received no external funding.

**Conflicts of Interest:** The authors declare no conflict of interest.

## Nomenclature

TRB	Tailor rolled blanks
VGR	Variable gauge rolling
TTZ	Thickness transition zone
DRF	Drop of rolling force
$\theta$	Bite angle in variable gauge rolling
$\alpha$	Bite angle in flat rolling
$\varphi$	Thickness transition zone wedge angle
$l_d$	Roll- specimen contact length
Thickness ratio	Thickness of the thinner side/thickness of the thicker side
$\Delta l$	Changes in contact length
$\bar{Y}$	Average yield stress
$\mu$	Friction coefficient
$w$	Width of tailor rolled blanks
$l_1$	Contact length in flat rolling
$l_2$	Contact length in downward rolling
$R$	Roll diameter

## References

1. Chuang, C.H.; Yang, R.J.; Li, G.; Mallela, K.; Pothurajo, P. Multidisciplinary design optimization on vehicle tailor rolled blank design. *Struct. Multidiscip. Optim.* **2008**, *35*, 551–560. [[CrossRef](#)]
2. Shafiei, E.; Dehghai, K. Tensile behavior of tailor rolled blanks with longitudinal thickness transition zone: Introducing a new tensile specimen. *Vacuum* **2017**, *143*, 71–86. [[CrossRef](#)]
3. Kopp, R.; Weidner, C.; Meyer, A. Flexibly rolled sheet metal and its use in sheet metal forming. *Adv. Mater. Res.* **2005**, *6–8*, 81–92. [[CrossRef](#)]
4. Meyer, A.; Weitbrock, B.; Hirt, G. Increasing of the drawing depth using tailored rolled blanks-numerical and experimental analysis. *Int. J. Mach. Tools Manuf.* **2008**, *48*, 522–531. [[CrossRef](#)]
5. Hirt, G.; Abratis, C.; Ames, J.; Meyer, A. Manufacturing of sheet metal parts from tailor rolled blanks. *J. Technol. Plast.* **2005**, *30*, 1–12.

6. Zhang, G.; Liu, X. Research on roll force for variable gauge rolling. *Adv. Mater. Res.* **2012**, *418–420*, 1232–1236. [[CrossRef](#)]
7. Shafiei, E.; Dehghani, K. Effects of thickness ratio and length of thickness transition zone on tensile behavior of tailor rolled blanks. *Trans. Indian Inst. Met.* **2018**, *71*, 1211–1222. [[CrossRef](#)]
8. Shafiei, E.; Dehghani, K. Effects of thickness ratio on tensile behavior of tailor rolled blanks. *Can. Metall. Q.* **2017**, *57*, 140–147. [[CrossRef](#)]
9. Ryabkov, N.; Jackel, F.; Vanputten, K.; Hirt, G. Production of blanks with thickness transitions in longitudinal and lateral direction through 3D-Strip Profile Rolling. *Int. J. Mater. Form.* **2008**, *1*, 391–394.
10. Duan, L.; Sun, G.; Cui, J.; Chen, T.; Chung, A.; Li, G. Crashworthiness design of vehicle structure with tailor rolled blank. *Struct. Multidiscip. Optim.* **2016**, *53*, 321–338. [[CrossRef](#)]
11. Sun, G.; Zhang, H.; Lu, G.; Guo, J.; Cui, J.; Li, Q. An experimental and numerical study on quasi-static and dynamic crashworthiness for tailor rolled blank (TRB) structures. *Mater. Des.* **2017**, *118*, 175–197.
12. Engler, O.; Shafer, G.; Brinkman, H.J.; Brecht, J.; Beiter, P.; Nijhof, K. Flexible rolling of aluminium alloy sheet—Process optimization and control of materials properties. *J. Mater. Proc. Technol.* **2016**, *229*, 139–148.
13. Beiter, P.; Gorche, P. On the development of novel light weight profiles for automotive industries by roll forming of tailor rolled blanks. *Key Eng. Mater.* **2011**, *473*, 45–52.
14. Zhang, H.W.; Liu, X.; Liu, L.Z.; Hu, P.; Wu, J. Study on nonuniform deformation of tailor rolled blanks during uniaxial tension. *Acta Metall. Sin.* **2015**, *28*, 1198–1204. [[CrossRef](#)]
15. Liu, X.; Wu, Z.; Zhi, F.; Zhang, G.; Zhi, Y. From TRB and LP to variable gauge rolling: Technology, theory, simulation and experiment. *Mater. Sci. Forum* **2012**, *706–709*, 1448–1453. [[CrossRef](#)]
16. Yu, H.L.; Lu, C.; Zhu, H.; Liu, X. The wave motion of the rolling force during variable gauge rolling. *Steel Res. Int.* **2013**, *84*, 1203–1208. [[CrossRef](#)]
17. Surender, K. *Technology of Metal Forming Processes*; Prentice Hall India: Delhi, India, 2011; ISBN 978-81-203-3425-0.
18. Lenard, J.G. Measurement of friction in cold flat rolling. *J. Mater. Shap. Technol.* **1991**, *9*. [[CrossRef](#)]



© 2018 by the authors. Licensee MDPI, Basel, Switzerland. This article is an open access article distributed under the terms and conditions of the Creative Commons Attribution (CC BY) license (<http://creativecommons.org/licenses/by/4.0/>).